Molecular Omics

ROYAL SOCIETY OF CHEMISTRY

RESEARCH ARTICLE

View Article Online
View Journal | View Issue

Cite this: *Mol. Omics*, 2020, **16**, 268

Identification of marker proteins of muscular dystrophy in the urine proteome from the *mdx-4cv* model of dystrophinopathy†

Stephen Gargan, [ab] Paul Dowling, [ab] Margit Zweyer, [c] Dieter Swandulla [d] and Kay Ohlendieck *[ab]

Received 11th December 2019,
Accepted 15th March 2020

DOI: 10.1039/c9mo00182d

rsc.li/molomics

Since the protein constituents of urine present a dynamic proteome that can reflect a variety of disease-related alterations in the body, the mass spectrometric survey of proteome-wide changes in urine promises new insights into pathogenic mechanisms. Urine can be investigated in a completely non-invasive way and provides valuable biomedical information on body-wide changes. In this report, we have focused on the urine proteome in X-linked muscular dystrophy using the established *mdx-4cv* mouse model of dystrophinopathy. In order to avoid potential artefacts due to the manipulation of the biofluid proteome prior to mass spectrometry, crude urine specimens were analyzed without the prior usage of centrifugation steps or concentration procedures. Comparative proteomics revealed 21 increased and 8 decreased proteins out of 870 identified urinary proteoforms using 50 μl of biofluid per investigated sample, *i.e.* 14 wild type *versus* 14 *mdx-4cv* specimens. Promising marker proteins that were almost exclusively found in *mdx-4cv* urine included nidogen, parvalbumin and titin. Interestingly, the mass spectrometric identification of urine-associated titin revealed a wide spread of peptides over the sequence of this giant muscle protein. The newly established urinomic signature of dystrophinopathy might be helpful for the design of non-invasive assays to improve diagnosis, prognosis, therapy-monitoring and evaluation of potential harmful side effects of novel treatments in the field of muscular dystrophy research.

Introduction

Measuring temporal changes in the protein composition of body fluids can be helpful for the systematic assessment and monitoring of body-wide effects due to physiological adaptations or pathological alterations. Biofluids present therefore an excellent starting point for the pathoproteomic analysis of disease processes, as long as the passive shedding or active secretion of tissue-associated proteins into the circulatory system can be measured by distinct variations in select protein species. In this respect, the increased usage of quantitative body fluid proteomics has greatly improved the scope of the bioanalytical analysis of protein release due to cellular damage.[1]

Besides serum and plasma samples, urine is one of the most frequently employed body fluids for the purpose of clinical diagnosis.[2] The advantage of using urine as a source of clinical marker molecules is the fact that this abundant biofluid can be obtained non-invasively and be sampled in a continuous way. The majority of urinary proteins originate from plasma components that pass through the glomerular filtration barrier, as well as liberated proteins from the kidney and urinary tract.[3–5]

Thus, in the absence of primary urological disease, the marked increase in distinct types of cellular proteins (that usually only exist in extremely low concentration in urine) presents an excellent way to identify novel proteomic biomarker candidates of body-wide tissue degeneration.[6] This is the reason why the protein composition of urine is an appropriate mirror of general health status and advanced urine protein analysis has an excellent potential to develop into an even more important diagnostic tool in modern medicine.[7] In the future, the optimum integration of highly sensitive and urine-based liquid biopsy techniques will ideally eliminate the need for invasive and potentially harmful tissue biopsy procedures or expensive imaging approaches in routine diagnostic, prognostic and therapy-monitoring methodologies.[8]

[a] *Department of Biology, Maynooth University, National University of Ireland, Maynooth W23F2H6, Co. Kildare, Ireland. E-mail: kay.ohlendieck@mu.ie; Fax: (+353) (1) 708-3845; Tel: (+353) (1) 708-3842*
[b] *Kathleen Lonsdale Institute for Human Health Research, Maynooth University, Maynooth W23F2H6, Co. Kildare, Ireland*
[c] *Department of Neonatology and Pediatric Intensive Care, Children's Hospital, University of Bonn, D-53113 Bonn, Germany*
[d] *Institute of Physiology II, University of Bonn, D-53115 Bonn, Germany*

† Electronic supplementary information (ESI) available. See DOI: 10.1039/c9mo00182d

Mass spectrometry-based proteomics has been instrumental for the establishment of the normal urinary proteome using a variety of protein separation and detection methods.[9–12] Several thousand urine-associated proteoforms have been cataloged.[10] The most abundant urinary proteins encompass 20 protein species, including the MUP class of major urinary proteins, albumin, serum enzymes and uromodulin. Approximately 200 proteins represent 95% of the urine proteome.[13] It therefore requires sophisticated mass spectrometric techniques to cover the considerable number of urine proteins with lower abundance.[14,15] In human urinomics, physiological parameters, gender and age are important parameters that have to be taken into account for the establishment of urinary protein signatures of diseases.[13,16,17]

In the field of muscular dystrophy research,[18] there is an urgent drive to identify novel biofluid markers for establishing improved diagnostic and therapy-monitoring approaches.[19–21] Duchenne muscular dystrophy, the most frequently inherited muscle wasting disease of early childhood,[22] is characterized by fibre necrosis, reactive myofibrosis and sterile inflammation in the skeletal musculature.[23–25] In addition to primary muscle weakness, dystrophinopathy is complicated by late-onset cardiomyopathy, respiratory impairments, neurological deficiencies, scoliosis and metabolic disturbances.[26–28] The genetic disorder is due to primary abnormalities in the extremely large *Dmd* gene, which encodes several isoforms of the protein dystrophin.[29] The full-length isoform of dystrophin, Dp427-M, functions in contractile fibres as a membrane cytoskeletal component and forms a supramolecular assembly with a variety of sarcolemma-associated proteins.[30] The dystrophin core complex, consisting of Dp427-M, dystroglycans, sarcoglycans, dystrobrevins, syntrophins and sarcospan, links the extracellular matrix component laminin to the intracellular actin cytoskeleton.[31] This *trans*-plasmalemmal structure plays a key role in lateral force transmission and the stabilization of the fibre surface during excitation-contraction-relaxation cycles.[32] In dystrophinopathy, the almost complete loss of Dp427-M causes a drastic reduction in the members of the dystrophin-associated glycoprotein complex,[33,34] which in turn triggers sarcolemmal micro-rupturing and calcium-induced proteolytic degradation.[35]

The proteomic screening of urine samples from dystrophic patients revealed the presence of N- and C-terminal fragments of the giant muscle protein titin.[36] Since X-linked muscular dystrophy is due to primary abnormalities in the membrane cytoskeletal protein dystrophin, changes in the sarcomeric protein titin might be linked to down-stream effects of the collapse of the dystrophin–glycoprotein complex.[30] The drastic elevation of urinary titin fragments was confirmed by immunoassays[37–39] and suggests that these protein species have a high potential as novel diagnostic markers and non-invasive screening tools.[21,40,41] Building on these findings, it was of interest to carry out a comprehensive proteomic comparison of urine and evaluate the body-wide effects of the dystrophic phenotype. In this report, we have used the established genetic *mdx-4cv* model of Duchenne muscular dystrophy,[42–44] which allows detailed comparisons of changes in the urine proteome due to primary or secondary pathological alterations in the dystrophic phenotype.[45–47]

Results and discussion

In order to improve our understanding of the molecular pathogenesis of dystrophinopathy and to identify novel protein candidates for the establishment of a proteomic biofluid signature of X-linked muscular dystrophy,[19–21] this study has focused on the mass spectrometric survey of the urine proteome from the dystrophic *mdx-4cv* mouse.

Dystrophin deficiency in the *mdx-4cv* model of dystrophinopathy

Prior to the proteomic profiling of urine samples, the mutant status of *mdx-4cv* skeletal muscle fibres was confirmed by immunofluorescence microscopy. As shown in Fig. 1, immuno-labelling

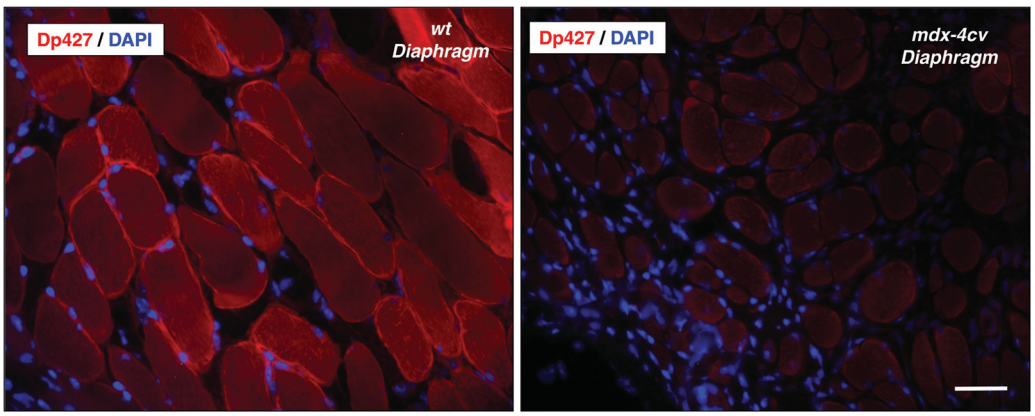

Fig. 1 Immunofluorescence microscopical characterization of the dystrophic diaphragm from the *mdx-4cv* mouse model of dystrophinopathy. Shown are transverse cryo-sections of wild type (*wt*) *versus* dystrophic *mdx-4cv* diaphragm muscle labelled with an antibody to the Dp427-M isoform of the membrane cytoskeletal dystrophin. Nuclei were counter-stained with the blue-fluorescent DNA dye 4′,6-diamidino-2-phenylindole (DAPI). The *mdx-4cv* muscle fibres are almost completely deficient of dystrophin at the sarcolemma. Bar equals 50 μm.

with an antibody to full-length dystrophin isoform Dp427-M demonstrated sarcolemmal localization in normal diaphragm and an almost complete absence of this membrane cytoskeletal protein in the dystrophic *mdx-4cv* diaphragm.

Proteomic profiling of urine

Urine contains a complex mixture of proteoforms over a wide dynamic concentration range.[5,9–11] In order to avoid the potential introduction of bioanalytical artefacts due to differential centrifugation procedures or extensive protein concentration steps, which are often used in urinomic investigations,[36] in this study neat urine specimens were analysed without any manipulation prior to mass spectrometry. The proteomic survey of wild type and *mdx-4cv* mouse urine samples identified 1010 and 870 protein species, respectively. Detailed information on proteomic multi-consensus data (4 files) and the raw data (28 files) of all identified urine proteins is available through the public repository Open Science Framework under the project title 'Proteomic profiling of mouse urine' (data identification number: 7dyqc; direct URL to data: https://osf.io/7dyqc/). The most abundant proteins in mouse urine that were mass spectrometrically identified in this study are listed in Table S1 (ESI†), including isoforms of major urinary protein, alpha-1-antitrypsin and alpha-amylase, as well as albumin, kallikrein, haptoglobin, serotransferrin, uromodulin and complement C3. The proteomic fingerprint of abundant urine-associated proteins is provided in Fig. S1 (ESI†), including the major urinary protein isoforms MUP1 to MUP20, isoforms of alpha-1-antitrypsin, alpha-amylase, haptoglobin and kallikrein.[10–13] The bioinformatic PANTHER analysis of protein families that were identified in mouse urine using mass spectrometry are presented in form of a pie chart in Fig. 2. This included a considerable number of cellular proteins, transporters, receptors, structural components, signalling proteins and various classes of enzymes, such as hydrolases, isomerases and oxidoreductases. The STRING-based interaction map of identified urine proteins is provided in Fig. S2 (ESI†).

Comparative proteomic profiling of urine from the *mdx-4cv* mouse model of dystrophinopathy

The comparative mass spectrometric profiling of *mdx-4cv* urine revealed 21 increased proteins (Table 1) and 8 decreased protein species (Table 2), whereby the extent of protein elevation was drastically higher as compared to the degree of a lowered abundance in specific proteins. The heat map of the urinomic analysis is provided in Fig. 3 and illustrates the differential expression pattern of changed proteins in wild type *versus* the dystrophic phenotype. Increased levels of the giant muscle protein titin in *mdx-4cv* urine, as previously reported in dystrophic patients and the conventional *mdx-23* mouse,[36–41] were clearly confirmed (Table 1). The proteomic screening study by Rouillon *et al.*,[36] which was carried out with urine samples from 5 Duchenne patients and 5 healthy subjects, lists 8 increased proteins (titin, uromodulin, nuclear transport factor NTF2, TNF receptor, myosin-1, fibulin-2, complement Clr, aminopeptidase) and 2 decreased proteins (cubulin, beta-galactosidase). Proteins in the study presented here were identified by a considerably higher number of unique peptides, especially in

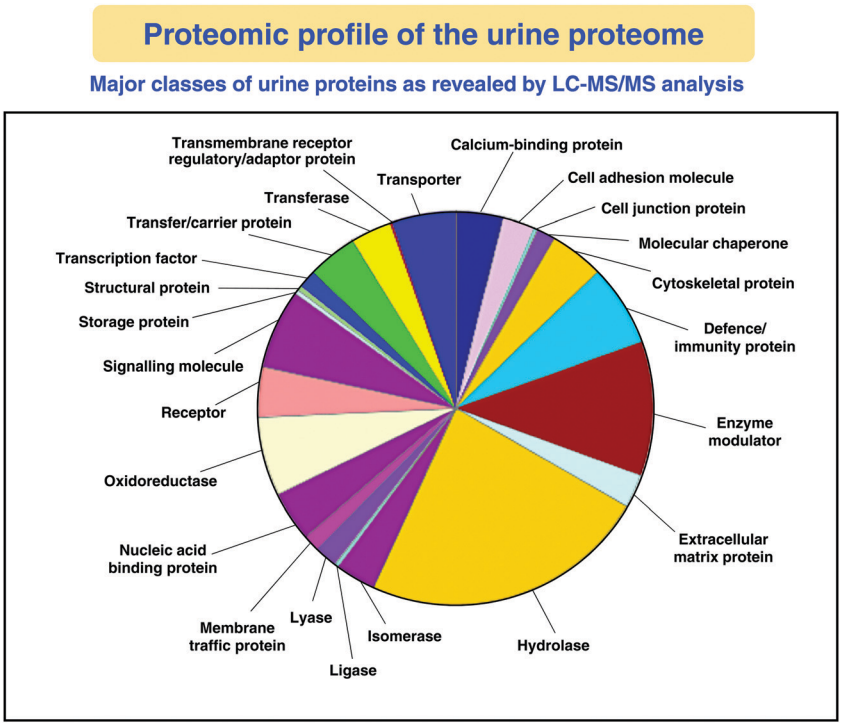

Fig. 2 Distribution of protein classes within the mouse urine proteome as determined by mass spectrometry-based proteomics and bioinformatic PANTHER analysis.

Table 1 Proteomic identification of increased proteins in urine from the *mdx-4cv* mouse model of Duchenne muscular dystrophy. The comparative proteomic survey was carried out with 28 urine samples from *mdx-4cv* (n = 7 biological repeats; n = 2 technical repeats) *versus* wild type (n = 7 biological repeats; n = 2 technical repeats) mice

Accession	Protein name	Gene	Coverage (%)	Unique peptides	ANOVA (p)	Fold change
A2ASS6	Titin	TTN	2.6	65	—	Detected only in *mdx*
O08539	Myc box-dependent-interacting protein 1	BIN1	17.7	6	—	Detected only in *mdx*
O88322	Nidogen-2	NID2	8.4	7	—	Detected only in *mdx*
P01942	Haemoglobin subunit alpha	HBA	36.6	5	—	Detected only in *mdx*
P04945	Ig kappa chain V–VI region	KV6AB	14.8	1	—	Detected only in *mdx*
P10493	Nidogen-1	NID1	10.3	10	—	Detected only in *mdx*
P32848	Parvalbumin alpha	PVALB	73.6	14	—	Detected only in *mdx*
Q9R045	Angiopoietin-related protein 2	ANGPTL2	18.3	10	—	Detected only in *mdx*
Q9DAK9	14 kDa phosphohistidine phosphatase	PHP14	45.9	6	0.000417	16.1
Q9D3H2	Odorant-binding protein 1a	OBP1A	49.7	8	0.002973	5.8
P62984	Ubiquitin-60S ribosomal protein L40	UBA52	43.0	9	3.21×10^{-5}	4.4
P01843	Ig lambda-1 chain C region	LAC1	61.9	4	4.59×10^{-7}	4.3
P01864	Ig gamma-2A chain C region	GCAB	17.3	5	0.040519	4.1
P29533	Vascular cell adhesion protein 1	VCAM1	33.3	2	4.81×10^{-7}	2.6
O88188	Lymphocyte antigen 86	LY86	33.3	4	1.26×10^{-6}	2.4
Q9WTR5	Cadherin-13	CDH13	26.2	12	0.005748	2.2
P01837	Immunoglobulin kappa constant	IGKC	38.7	6	0.001230	2.1
P01898	H-2 class I histocompatibility antigen, Q10 alpha chain	H2-Q10	43.4	10	0.000233	2.1
P11276	Fibronectin	FN1	17.8	27	0.000837	1.7
Q07456	Protein AMBP	AMBP	41.3	15	0.000129	1.7
P04939	Major urinary protein 3	MUP3	72.3	14	0.039672	1.6

Table 2 Proteomic identification of decreased proteins in urine from the *mdx-4cv* mouse model of Duchenne muscular dystrophy. The comparative proteomic survey was carried out with 28 urine samples from *mdx-4cv* (n = 7 biological repeats; n = 2 technical repeats) *versus* wild type (n = 7 biological repeats; n = 2 technical repeats) mice

Accession	Protein name	Gene	Coverage (%)	Unique peptides	ANOVA (p)	Fold change
Q02819	Nucleobindin-1	NUCB1	46.84	17	0.018151	2.9
P23953	Carboxylesterase 1C	CES1C	31.59	12	0.011188	2.2
P09470	Angiotensin-converting enzyme	ACE	19.66	19	1.61×10^{-5}	2.1
O09159	Lysosomal alpha-mannosidase	MAN2B1	16.29	14	0.037992	2.1
Q5SSE9	ATP-binding cassette sub-family A member 13	ABCA13	11.25	33	0.042472	1.7
Q61147	Ceruloplasmin	CP	21.77	15	0.002404	1.7
Q06890	Clusterin	CLU	33.48	18	1.36×10^{-5}	1.7
P00688	Pancreatic alpha-amylase	AMY2	53.15	15	0.007610	1.6

the case of titin. As shown in the diagrammatic presentation of the proteomic fingerprints of a select number of elevated proteins in *mdx-4cv* urine (Fig. S3 (ESI†) and Fig. 4a), the mass spectrometric analysis of urine-associated titin revealed a widespread presence of 65 unique peptides over the entire sequence of this giant muscle protein (Fig. S4, ESI†). Immunoblotting confirmed the drastic increase of titin fragments in *mdx-4cv* urine as shown in Fig. 4c–e. Titin is one of the most abundant sarcomeric muscle proteins and despite its extremely large size is routinely identified by a sequence coverage of above 50% in crude muscle extracts (Fig. 4b) using proteomics.[48] Increased titin levels in *mdx-4cv* urine correlate well with the previous proteomic identification of a higher concentration of titin in *mdx-4cv* and *mdx-23* serum.[19,49]

Therefore, the loss of dystrophin and its associated glycoprotein complex appears to destabilize contractile fibres by impairing the *trans*-sarcolemmal linkage between the intracellular actin cytoskeleton and the extracellular matrix component laminin.[30] Ca^{2+}-Induced protein degradation and progressive weakening of the cytoskeletal network appear to have a direct effect on the structural and functional integrity of the sarcomeric apparatus and cause the release of titin fragments. In normal muscle, the half-sarcomere spanning titin isoforms with a molecular mass of over 3 MDa were shown to interact with their carboxy-terminus at the M-band and the amino-terminal region extends this tight molecular coupling to the Z-disk. Titin is intrinsically involved in sarcomeric protein scaffolding and cellular signalling mechanisms. This includes the critical cellular processes of myofibrillar assembly during myogenesis and the functioning as a molecular spring that determines passive stretch within myocytes, as well as critical aspects of signal integration and mechano-sensing as a regulatory node of contractile fibres.[48] These processes appear to be interrupted in X-linked muscular dystrophy due to the deficiency in dystrophin and the accompanying degradation of sarcomeric titin. The subsequent release of titin fragments into circulation is reflected by elevated levels of titin peptides in *mdx-4cv* urine.

In addition to titin, promising marker proteins that are possibly linked to muscle degeneration and were shown here to be drastically increased in *mdx-4cv* urine, include parvalbumin, nidogen isoforms NID1 and NID2, the myc box-dependent interacting protein BIN1, angiopoietin-related protein 2, cadherin-13

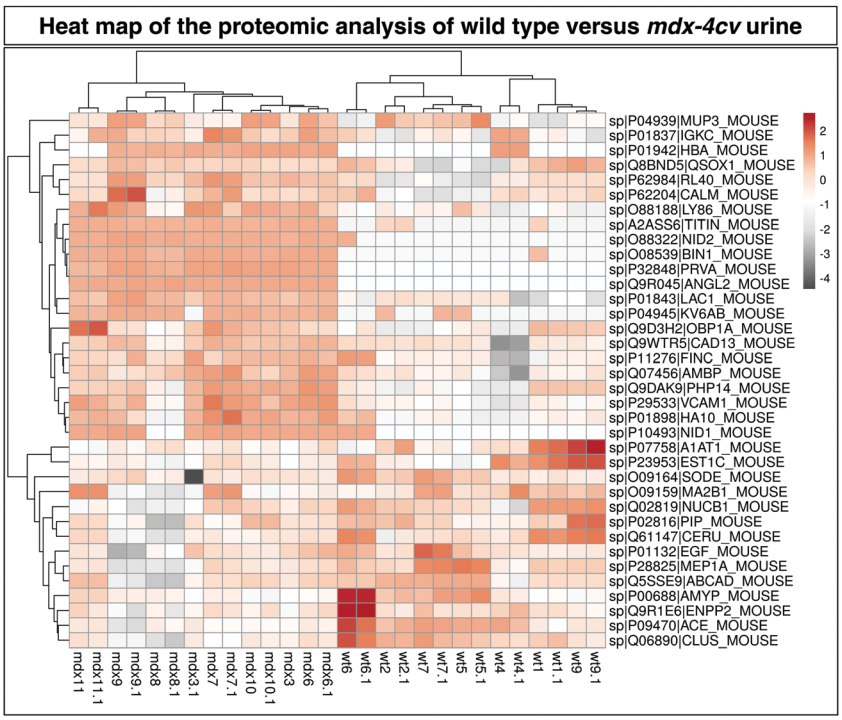

Fig. 3 Heat map of the urinomic analysis of changed proteins in wild type *versus* the *mdx-4cv* mouse model of dystrophinopathy. The comparative proteomic survey was carried out with 28 urine samples from *mdx-4cv* (n = 7 biological repeats; n = 2 technical repeats) *versus* wild type (n = 7 biological repeats; n = 2 technical repeats) mice.

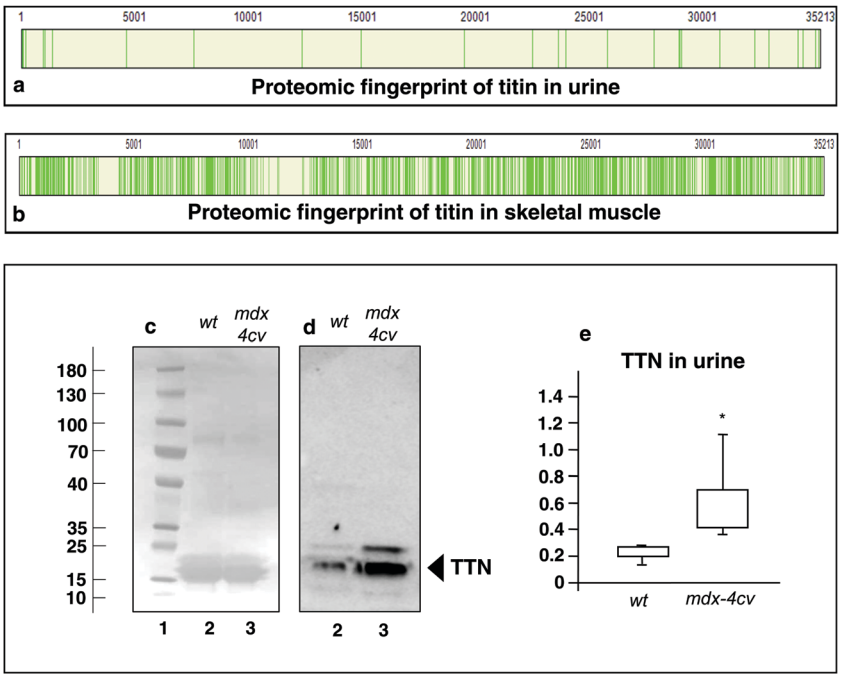

Fig. 4 Proteomic fingerprint and immunoblot analysis of titin in urine from wild type *versus* dystrophic mice. Shown are the proteomic fingerprints of the giant protein species titin (TTN) in urine (a) *versus* skeletal muscle (b). The green bars represent peptide sequences that were identified by mass spectrometry-based proteomics. In the lower panels are shown protein blots of wild type *versus* *mdx-4cv* urine samples stained with Ponceau Red (c) and an immunoblot labelled with an antibody to titin (d). Lanes 1–3 contain molecular mass standards, wild type urine and *mdx-4cv* urine, respectively. In panel (e) is shown the statistical analysis of titin immunoblotting (Mann–Whitney U test; p = 0.01208; n = 5). The value of molecular mass standards ($\times 10^{-3}$ kDa) is marked on the left side of the blots.

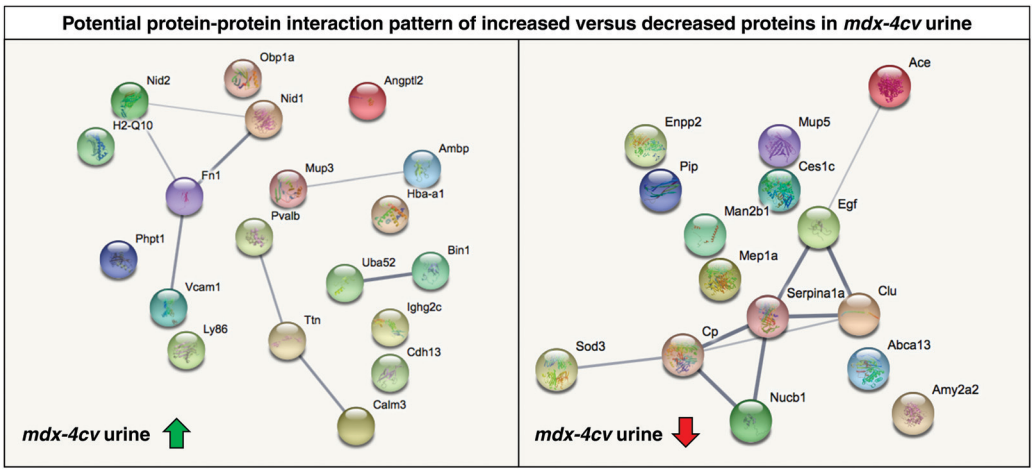

Fig. 5 Bioinformatic STRING analysis of potential protein–protein interactions of increased *versus* decreased proteins in urine from the *mdx-4cv* mouse model of dystrophinopathy, as summarized in the heat map of Fig. 3.

and fibronectin (Table 1 and Fig. S3, ESI†). Parvalbumin was also shown to be elevated in *mdx-23* serum[49] and greatly reduced in various muscle types, including *flexor digitorum brevis*, *interosseous* and the highly fibrotic diaphragm in the *mdx-23* and *mdx-4cv* mouse.[50–53] Hence, the changes in this cytosolic Ca^{2+}-binding protein that exists predominantly in mature fast-twitching fibers, might be due to a dystrophin-deficient and leaky sarcolemma membrane. Micro-rupturing of the plasma membrane appears to trigger a substantial release of parvalbumin into the circulation.[49,54] and this might explain the greatly increased presence of this muscle-derived protein in *mdx-4cv* urine. Interestingly, the nidogen isoform NID1, which is a laminin-associated glycoprotein of the basement membrane, was previously shown to be increased in *mdx-23* serum[55] and decreased in *mdx-23* heart.[56] Thus, the elevated concentration of nidogen in *mdx-4cv* urine might be related to shedding of this extracellular protein from fibrotic heart cells in association with dystrophinopathy-related cardiomyopathy. Of note, increased levels of fibronectin were also established in dystrophic and fibrotic *mdx-4cv* diaphragm muscle[57] and serum specimens from Duchenne patients.[58] Reactive myofibrosis might therefore be linked to increased release of fibronectin into the circulatory system and explain its elevated concentration in *mdx-4cv* urine.

Interesting urine-associated proteins with a decreased abundance were identified as the Ca^{2+}-binding protein nucleobindin of the Golgi apparatus and carboxylesterase, angiotensin-converting enzyme and lysosomal alpha-mannosidase. Potential protein–protein interaction patterns of identified proteins are illustrated in the bioinformatic STRING analysis of Fig. 5. Protein clusters of interest are represented by increases in the titin–parvalbumin hub and the extracellular fibronectin–nidogen axis, as well as decreases in the alpha-1-antitrypsin–epidermal growth factor–ceruloplasmin hub. The mass spectrometric survey of proteome-wide changes in *mdx-4cv* urine has therefore provided (i) new insights into pathogenic mechanisms of muscular dystrophy, (ii) confirmed the drastically elevated levels of titin and fibronectin in urine from the dystrophic phenotype, and (iii) identified novel potential disease markers in an easily accessible biofluid, including the cytosolic protein parvalbumin and the extracellular matrix component nidogen.

The potential of urine as a biofluid for non-invasive and systemic sampling approaches in muscular dystrophy research

Urine is characterized by a complex set of protein constituents with a wide concentration range.[5,10] Dynamic changes in the urine proteome may reflect a variety of physiological adaptations or disease-associated alterations in the body,[6–8] making this abundant biofluid an excellent starting point for detailed omics-type investigations. Proteome-wide changes in urine are an ideal source for a better understanding of the complex molecular and cellular pathogenesis of inherited diseases, such as Duchenne muscular dystrophy.[21] One of the great advantages of urine over invasive tissue biopsy procedures or minimally invasive serum sampling is the fact that this biofluid can be harvested in a completely non-invasive way to provide meaningful biomedical information on body-wide changes in a continuous manner.[11–13] For example, in cases of acute muscle damage that results in rhabdomyolysis,[59] the release of the contents of injured myofibers into the circulatory system is reflected by a marked elevation of urine myoglobin.[60] In analogy to urine myoglobin as a muscle damage marker for the risk assessment of acute renal failure following rhabdomyolysis, dystrophinopathy-related changes in the urine protein profile established in this report might serve as a useful addition to the biofluid marker signature of X-linked muscular dystrophy.

Conclusion

The systematic mass spectrometric survey of the urine proteome from wild type *versus* dystrophic *mdx-4cv* mice has identified a considerable number of changed protein species. Especially the elevated levels of titin, parvalbumin, nidogen, cadherin and fibronectin present interesting biomarker candidates in

association with chronic muscle wasting and reactive myofibrosis. Thus, in the absence of urological pathology, urine sampling presents an ideal source for carrying out non-invasive liquid biopsies as an alternative to highly invasive muscle biopsy procedures. In the long-term, the newly established proteomic signature of urine-associated changes in association with X-linked muscular dystrophy might be helpful for the improved design of simplified assays for diagnostic and prognostic purposes, as well as therapy-monitoring and the continuous evaluation of potential side effects of novel treatments of dystrophinopathy, such as exon skipping, stop codon read-through, viral gene transfer, stem cell/myoblast transfer, utrophin replacement or CRISPR/Cas9 genome editing.[61–64] Since novel treatment protocols, such as gene therapy, are routinely tested in genetic mouse models prior to clinical trials,[44] the findings from our new study on the *mdx-4cv* model should be a helpful addition to the class of non-invasive marker proteins to evaluate new approaches to treat dystrophinopathy. Ideally, combinations of proteomic and metabolomic urine-based biomarkers[65] would be used for the systems biological assessment of the molecular pathogenesis of dystrophinopathy.

Materials and methods

Materials

Materials and general analytical-grade reagents were obtained from GE Healthcare (Little Chalfont, Buckinghamshire, UK), BioRad Laboratories (Hemel-Hempstead, Hertfordshire, UK) and Sigma Chemical Company (Dorset, UK). For the filter-aided sample preparation method FASP, Vivacon 500 (30 000 MWCO, product number: VN0H22) spin filters were acquired from Sartorius (Göttingen, Germany). Sequencing grade-modified trypsin, Lys-C and Protease Max Surfactant Trypsin Enhancer were obtained from Promega (Madison, WI, USA). Protease inhibitors were purchased from Roche Diagnostics (Mannheim, Germany). The Pierce 660 nm Protein Assay Reagent was from ThermoFisher Scientific (Dublin, Ireland). For immunofluorescence microscopy and immunoblotting, primary antibodies were obtained from NovoCastra, Leica Biosystems, Newcastle Upon Tyne, UK (NCL-Dys2 to the carboxy terminus of dystrophin isoform Dp427-M) and Sigma Chemical Company, Dorset, UK (mAb T11, T9030 to titin). Chemicon International (Temecula, CA, USA) provided peroxidase-conjugated secondary antibodies. Normal goat serum and goat anti-mouse IgG RRX (Rhodamine Red-X) were purchased from Molecular Probes, Life Technologies (Darmstadt, Germany) and Jackson ImmunoResearch (West Grove, PA, USA), respectively.

Urine and muscle specimens from the *mdx-4cv* mouse model of dystrophinopathy

The sampling of urine and harvesting of *post-mortem* muscle tissue samples was carried out according to institutional regulations. All mice were handled in strict adherence to local governmental and institutional animal care regulations and were approved by the Institutional Animal Care and Use Committee (Amt für Umwelt, Verbraucherschutz und Lokale Agenda der Stadt Bonn, North Rhine-Westphalia, Germany). Comparative biofluid proteomics was carried out by standardized procedures, as previously described in detail.[49,66] Fresh urine specimens were collected from 12 month old dystrophic *mdx-4cv* mice and age-matched wild type C57BL/6 mice through the Bioresource Unit of the University of Bonn,[46] where animals were kept under standard conditions according to German legislation on the use of animals in experimental research. Commonly used procedures to sample urine from small rodents, such as abdominal pressure or urinary catheterization,[36] was not applied in this study. Parallel to urine sampling, skeletal muscle specimens were dissected and prepared for immunofluorescence microscopical comparison between wild type and dystrophic mice. The collected urine samples were immediately quick-frozen in liquid nitrogen and then transported on dry ice to Maynooth University in accordance with the Department of Agriculture (animal by-product register number 2016/16 to the Department of Biology, National University of Ireland, Maynooth). Samples were stored at −80 °C prior to proteomic analysis.

Proteolytic digestion of urine proteins

The protein concentration of 50 μL urine samples was equalized with label-free solubilisation buffer (6 M urea, 2 M thiourea, 10 mM Tris, pH 8.0 in LC-MS grade water). The Pierce 660 nm protein assay system was used to determine protein concentration.[67] This assay has previously been used to determine the concentration of urine protein.[68] Suspensions were then buffer exchanged using the filter-aided sample preparation (FASP) method in a buffer containing 8 M urea/50 mM NH_4HCO_3/0.1% ProteaseMax, as described in detail by Wiśniewski.[69] After reduction with dithiothreitol and iodoacetic acid-mediated alkylation, a double digestion was performed using Lys-C (for 4 hours at 37 °C) and trypsin (overnight at 37 °C) on 5 μg of urinary protein. Digested samples were desalted prior to analysis using C18 spin columns (Thermo Scientific, UK), dried through vacuum centrifugation and re-suspended in mass spectrometry loading buffer (2% acetonitrile (ACNA)(ACN), 0.05% trifluoroacetic acid (TFA) in LC-MS grade water).[46] Peptides were vortexed, sonicated and briefly centrifuged at 14 000×*g* and the supernatant transferred to mass spectrometry vials for label-free liquid chromatography mass spectrometry (LC-MS/MS),[53] a robust and reliable method for the comparative analysis of protein expression patterns.[70–72] Both, label-free and label-based strategies exhibit comparable levels of reproducibility in relation to protein quantification. Label-free mass spectrometry was shown to provide excellent peptide sequence coverage and the detection of a large number of differentially expressed protein species.[73,74]

Label-free liquid chromatography mass spectrometry

For the comparative proteomic survey of urine samples from *mdx-4cv* (n = 7 biological repeats; n = 2 technical repeats) *versus* wild type (n = 7 biological repeats; n = 2 technical repeats) mice, 500 ng of each digested sample was loaded onto a Q-Exactive high-resolution accurate mass spectrometer connected to a

Dionex Ultimate 3000 (RSLCnano) chromatography system (ThermoFisher Scientific, Hemel Hempstead, UK). Sample loading was carried out by an auto-sampler onto a C18 trap column (C18 PepMap, 300 μm id × 5 mm, 5 μm particle size, 100 Å pore size; Thermo Fisher Scientific). The trap column was switched on-line with an analytical Biobasic C18 Picofrit column (C18 PepMap, 75 μm id × 50 cm, 2 μm particle size, 100 Å pore size; Dionex). Peptides were eluted over a 65 minute binary gradient [solvent A: 2% (v/v) ACN and 0.1% (v/v) formic acid in LC-MS grade water and solvent B: 80% (v/v) ACN and 0.1% (v/v) formic acid in LC-MS grade water]: 3% solvent B for 5 minutes, 3–10% solvent B for 5 minutes, 10–40% solvent B for 30 minutes, 40–90% solvent B for 5 minutes, 90% solvent B for 5 minutes and 3% solvent B for 10 minutes.[47] The column flow rate was set to 0.3 μL min^{-1}. Data were acquired with Xcalibur software (Thermo Fisher Scientific). The mass spectrometer was externally calibrated and operated in positive, data-dependent mode. A full survey MS scan was performed in the 300–1700 *m*/*z* range with a resolution of 140 000 (*m*/*z* 200) and a lock mass of 445.12003. Collision-induced dissociation (CID) fragmentation was carried out with the fifteen most intense ions per scan and at 17 500 resolution. Within 30 seconds a dynamic exclusion window was applied. An isolation window of 2 *m*/*z* and one microscan were used to collect suitable tandem mass spectra.

Protein identification and quantification

Data analysis, processing and visualisation for urine protein identification and label-free quantification (LFQ) normalisation of MS/MS data was performed using MaxQuant v1.5.2.8 (http://www.maxquant.org) and Perseus v.1.5.6.0 (www.maxquant.org/) software. Differential protein expression patterns in the *mdx-4cv versus* wild type urinary proteomes were initially identified using Proteome Discoverer 1.4 against Sequest HT (SEQUEST HT algorithm, licence Thermo Scientific, registered trademark University of Washington, USA) using the UniProtKB/Swiss-Prot database for *Mus musculus*. The following search parameters were used for protein identification: (i) peptide mass tolerance set to 10 ppm, (ii) MS/MS mass tolerance set to 0.02 Da, (iii) an allowance of up to two missed cleavages, (iv) carbamidomethylation set as a fixed modification and (v) methionine oxidation set as a variable modification. Peptides were filtered using a minimum XCorr score of 1.5 for 1, 2.0 for 2, 2.25 for 3 and 2.5 for 4 charge states, with peptide probability set to high confidence. XCorr is a search-dependent score employed by the SEQUEST HT search engine in Proteome Discoverer, and reflects the number of fragment ions that are common to two different peptides with the same precursor mass. Since the XCorr value is dependent upon the number of identified fragment ions, its value is usually higher for larger peptides. XCorr scores are filtered based on charge state, whereby larger XCorr thresholds are used for higher charge states. For quantitative analysis, samples were evaluated with MaxQuant software and the Andromeda search engine used to explore the detected features against the UniProtKB/SwissProt database for *Mus musculus.* The following search parameters were used: (i) first search peptide tolerance of 20 ppm, (ii) main search peptide tolerance of 4.5 ppm, (iii) cysteine carbamidomethylation set as a fixed modification, (iv) methionine oxidation set as a variable modification, (v) a maximum of two missed cleavage sites and (vi) a minimum peptide length of seven amino acids. The false discovery rate (FDR) was set to 1% for both peptides and proteins using a target-decoy approach. Relative quantification was performed using the MaxLFQ algorithm. The ''proteinGroups.txt'' file produced by MaxQuant was further analysed in Perseus. Proteins that matched to the reverse database or a contaminants database or that were only identified by site were removed. The LFQ intensities were log2 transformed, and only proteins found in all seven replicates in at least one group were used for further analysis. Data imputation was performed to replace missing values with values that simulate signals from peptides with low abundance chosen from a normal distribution specified by a downshift of 1.8 times the mean standard deviation of all measured values and a width of 0.3 times this standard deviation. A two-sample *t*-test was performed using $p < 0.05$ on the post imputated data to identify statistically significant differentially abundant proteins. The freely available software packages PANTHER[75] (http://pantherdb.org/) and STRING[76] (https://string-db.org/) were used to identify protein classes and characterise potential protein interactions, respectively.

Immunofluorescence microscopy and immunoblot analysis

Microscopical procedures were carried out as previously described in detail.[45] Transverse diaphragm muscle sections of 10 μm thickness from wild type and dystrophic *mdx-4cv* mice were incubated overnight at 4 °C with an appropriately diluted primary antibody to dystrophin isoform Dp427-M. Following washing with phosphate-buffered saline and incubation with fluorescently-labelled secondary antibodies, as well as counter-staining of nuclei, muscle tissue sections were examined under a Zeiss Axioskop 2 epifluorescence microscope equipped with a digital Zeiss AxioCam HRc camera (Carl Zeiss Jena GmbH, Jena, Germany). Comparative immunoblotting was used as an orthogonal method for the independent verification of changes in urine-associated titin in the *mdx-4cv* mouse and carried out by an optimized method.[46]

Conflicts of interest

There are no conflicts to declare.

Acknowledgements

Research was supported by funding from the Kathleen Lonsdale Institute for Human Health Research at Maynooth University. The Q-Exactive quantitative mass spectrometer was funded under the Research Infrastructure Call 2012 by Science Foundation Ireland (SFI-12/RI/2346/3).

References

1 É. Csősz, G. Kalló, B. Márkus, E. Deák, A. Csutak and J. Tőzsér, Quantitative body fluid proteomics in

medicine – A focus on minimal invasiveness, *J. Proteomics*, 2017, **153**, 30–43.
2 N. A. Brunzel, *Fundamentals of Urine and Body Fluid Analysis*, Elsevier/Saunders, St. Louis, MO, 4th edn, 2016.
3 L. Zou and W. Sun, Human urine proteome: a powerful source for clinical research, *Adv. Exp. Med. Biol.*, 2015, **845**, 31–42.
4 A. Beasley-Green, Urine Proteomics in the Era of Mass Spectrometry, *Int. Neurourol. J.*, 2016, **20**, S70–S75.
5 M. Zhao, M. Li, Y. Yang, Z. Guo, Y. Sun, C. Shao, M. Li, W. Sun and Y. Gao, A comprehensive analysis and annotation of human normal urinary proteome, *Sci. Rep.*, 2017, **7**, 3024.
6 S. Thomas, L. Hao, W. A. Ricke and L. Li, Biomarker discovery in mass spectrometry-based urinary proteomics, *Proteomics Clin Appl*, 2016, **10**, 358–370.
7 K. Fischer, Urinary marker-old wine in new bottles?, *Urologe*, 2018, **57**, 1040–1047.
8 E. Rodríguez-Suárez, J. Siwy, P. Zürbig and M. Mischak, Urine as a source for clinical proteome analysis: from discovery to clinical application, *Biochim. Biophys. Acta*, 2014, **1844**, 884–898.
9 A. Marimuthu, R. N. O'Meally, R. Chaerkady, Y. Subbannayya, V. Nanjappa, P. Kumar, D. S. Kelkar, S. M. Pinto, R. Sharma, S. Renuse, R. Goel, R. Christopher, B. Delanghe, R. N. Cole, H. C. Harsha and A. Pandey, A comprehensive map of the human urinary proteome, *J. Proteome Res.*, 2011, **10**, 2734–2743.
10 L. Santucci, G. Candiano, A. Petretto, M. Bruschi, C. Lavarello, E. Inglese, P. G. Righetti and G. M. Ghiggeri, From hundreds to thousands: Widening the normal human Urinome (1), *J. Proteomics*, 2015, **112**, 53–62.
11 L. Santucci, M. Bruschi, G. Candiano, F. Lugani, A. Petretto, A. Bonanni and G. M. Ghiggeri, Urine Proteome Biomarkers in Kidney Diseases. I. Limits, Perspectives, and First Focus on Normal Urine, *Biomarker Insights*, 2016, **11**, 41–48.
12 S. Filip, J. Zoidakis, A. Vlahou and H. Mischak, Advances in urinary proteome analysis and applications in systems biology, *Bioanalysis*, 2014, **6**, 2549–2569.
13 N. Nagaraj and M. Mann, Quantitative analysis of the intra- and inter-individual variability of the normal urinary proteome, *J. Proteome Res.*, 2011, **10**, 637–645.
14 N. Khristenko and B. Domon, Quantification of proteins in urine samples using targeted mass spectrometry methods, *Methods Mol. Biol.*, 2015, **1243**, 207–220.
15 M. Harpole, J. Davis and V. Espina, Current state of the art for enhancing urine biomarker discovery, *Expert Rev. Proteomics*, 2016, **13**, 609–626.
16 C. Shao, M. Zhao, X. Chen, H. Sun, Y. Yang, X. Xiao, Z. Guo, X. Liu, Y. Lv, X. Chen, W. Sun, D. Wu and Y. Gao, Comprehensive Analysis of Individual Variation in the Urinary Proteome Revealed Significant Gender Differences, *Mol. Cell. Proteomics*, 2019, **18**, 1110–1122.
17 J. Wu and Y. Gao, Physiological conditions can be reflected in human urine proteome and metabolome, *Expert Rev. Proteomics*, 2015, **12**, 623–636.
18 E. Mercuri, C. G. Bönnemann and F. Muntoni, Muscular dystrophies, *Lancet*, 2019, **394**, 2025–2038.
19 Y. Hathout, H. Seol, M. H. Han, A. Zhang, K. J. Brown and E. P. Hoffman, Clinical utility of serum biomarkers in Duchenne muscular dystrophy, *Clin. Proteomics*, 2016, **13**, 9.
20 S. Murphy, M. Zweyer, R. R. Mundegar, D. Swandulla and K. Ohlendieck, Proteomic serum biomarkers for neuromuscular diseases, *Expert Rev. Proteomics*, 2018, **15**, 277–291.
21 P. Dowling, S. Murphy, M. Zweyer, M. Raucamp, D. Swandulla and K. Ohlendieck, Emerging proteomic biomarkers of X-linked muscular dystrophy, *Expert Rev. Mol. Diagn.*, 2019, **19**, 739–755.
22 J. K. Mah, L. Korngut, K. M. Fiest, J. Dykeman, L. J. Day, T. Pringsheim and N. Jette, A Systematic Review and Meta-analysis on the Epidemiology of the Muscular Dystrophies, *Can. J. Neurol. Sci.*, 2016, **43**, 163–177.
23 J. Shin, M. M. Tajrishi, Y. Ogura and A. Kumar, Wasting mechanisms in muscular dystrophy, *Int. J. Biochem. Cell Biol.*, 2013, **45**, 2266–2279.
24 A. Holland, S. Murphy, P. Dowling and K. Ohlendieck, Pathoproteomic profiling of the skeletal muscle matrisome in dystrophinopathy associated myofibrosis, *Proteomics*, 2016, **16**, 345–366.
25 J. G. Tidball, S. S. Welc and M. Wehling-Henricks, Immunobiology of Inherited Muscular Dystrophies, *Compr. Physiol.*, 2018, **8**, 1313–1356.
26 J. D. Hsu and R. Quinlivan, Scoliosis in Duchenne muscular dystrophy (DMD), *Neuromuscular Disord.*, 2013, **23**, 611–617.
27 V. Ricotti, W. P. Mandy, M. Scoto, M. Pane, N. Deconinck, S. Messina, E. Mercuri, D. H. Skuse and F. Muntoni, Neurodevelopmental, emotional, and behavioural problems in Duchenne muscular dystrophy in relation to underlying dystrophin gene mutations, *Dev. Med. Child Neurol.*, 2016, **58**, 77–84.
28 D. J. Birnkrant, K. Bushby, C. M. Bann, B. A. Alman, S. D. Apkon, A. Blackwell, L. E. Case, L. Cripe, S. Hadjiyannakis, A. K. Olson, D. W. Sheehan, J. Bolen, D. R. Weber and L. M. Ward, DMD Care Considerations Working Group, Diagnosis and management of Duchenne muscular dystrophy, part 2: respiratory, cardiac, bone health, and orthopaedic management, *Lancet Neurol.*, 2018, **17**, 347–361.
29 S. Guiraud, A. Aartsma-Rus, N. M. Vieira, K. E. Davies, G. J. van Ommen and L. M. Kunkel, The Pathogenesis and Therapy of Muscular Dystrophies, *Annu. Rev. Genomics Hum. Genet.*, 2015, **16**, 281–308.
30 S. Murphy and K. Ohlendieck, The biochemical and mass spectrometric profiling of the dystrophin complexome from skeletal muscle, *Comput. Struct. Biotechnol. J.*, 2015, **14**, 20–27.
31 J. M. Ervasti and K. J. Sonnemann, Biology of the striated muscle dystrophin-glycoprotein complex, *Int. Rev. Cytol.*, 2008, **265**, 191–225.
32 K. Ohlendieck, Towards an understanding of the dystrophin-glycoprotein complex: linkage between the extracellular matrix and the membrane cytoskeleton in muscle fibers, *Eur. J. Cell Biol.*, 1996, **69**, 1–10.
33 J. M. Ervasti, K. Ohlendieck, S. D. Kahl, M. G. Gaver and K. P. Campbell, Deficiency of a glycoprotein component of

the dystrophin complex in dystrophic muscle, *Nature*, 1990, **345**, 315–319.

34 K. Ohlendieck, K. Matsumura, V. V. Ionasescu, J. A. Towbin, E. P. Bosch, S. L. Weinstein, S. W. Sernett and K. P. Campbell, Duchenne muscular dystrophy: deficiency of dystrophin-associated proteins in the sarcolemma, *Neurology*, 1993, **43**, 795–800.

35 A. Holland, S. Carberry and K. Ohlendieck, Proteomics of the dystrophin-glycoprotein complex and dystrophinopathy, *Curr. Protein Pept. Sci.*, 2013, **14**(8), 680–697.

36 J. Rouillon, A. Zocevic, T. Leger, C. Garcia, J. M. Camadro, B. Udd, B. Wong, L. Servais, T. Voit and F. Svinartchouk, Proteomics profiling of urine reveals specific titin fragments as biomarkers of Duchenne muscular dystrophy, *Neuromuscular Disord.*, 2014, **24**, 563–573.

37 N. Maruyama, T. Asai, C. Abe, A. Inada, T. Kawauchi, K. Miyashita, M. Maeda, M. Matsuo and Y. I. Nabeshima, Establishment of a highly sensitive sandwich ELISA for the N-terminal fragment of titin in urine, *Sci. Rep.*, 2016, **6**, 39375.

38 A. S. Robertson, M. J. Majchrzak, C. M. Smith, R. C. Gagnon, N. Devidze, G. B. Banks, S. C. Little, F. Nabbie, D. I. Bounous, J. DiPiero, L. K. Jacobsen, L. J. Bristow, M. K. Ahlijanian and S. A. Stimpson, Dramatic elevation in urinary amino terminal titin fragment excretion quantified by immunoassay in Duchenne muscular dystrophy patients and in dystrophin deficient rodents, *Neuromuscular Disord.*, 2017, **27**, 635–645.

39 H. Awano, M. Matsumoto, M. Nagai, T. Shirakawa, N. Maruyama, K. Iijima, Y. I. Nabeshima and M. Matsuo, Diagnostic and clinical significance of the titin fragment in urine of Duchenne muscular dystrophy patients, *Clin. Chim. Acta*, 2018, **476**, 111–116.

40 M. Matsuo, T. Shirakawa, H. Awano and H. Nishio, Receiver operating curve analyses of urinary titin of healthy 3-y-old children may be a noninvasive screening method for Duchenne muscular dystrophy, *Clin. Chim. Acta*, 2018, **486**, 110–114.

41 M. Matsuo, H. Awano, N. Maruyama and H. Nishio, Titin fragment in urine: A noninvasive biomarker of muscle degradation, *Adv. Clin. Chem.*, 2019, **90**, 1–23.

42 W. B. Im, S. F. Phelps, E. H. Copen, E. G. Adams, J. L. Slightom and J. S. Chamberlain, Differential expression of dystrophin isoforms in strains of mdx mice with different mutations, *Hum. Mol. Genet.*, 1996, **5**, 1149–1153.

43 E. D. Tichy and F. Mourkioti, A new method of genotyping MDX4CV mice by PCR-RFLP analysis, *Muscle Nerve*, 2017, **56**, 522–524.

44 N. E. Bengtsson, J. K. Hall, G. L. Odom, M. P. Phelps, C. R. Andrus, R. D. Hawkins, S. D. Hauschka, J. R. Chamberlain and J. S. Chamberlain, Muscle-specific CRISPR/Cas9 dystrophin gene editing ameliorates pathophysiology in a mouse model for Duchenne muscular dystrophy, *Nat. Commun.*, 2017, **8**, 14454.

45 S. Murphy, P. Dowling, M. Zweyer, R. R. Mundegar, M. Henry, P. Meleady, D. Swandulla and K. Ohlendieck, Proteomic analysis of dystrophin deficiency and associated changes in the aged mdx-4cv heart model of dystrophinopathy-related cardiomyopathy, *J. Proteomics*, 2016, **145**, 24–36.

46 S. Murphy, M. Zweyer, M. Henry, P. Meleady, R. R. Mundegar, D. Swandulla and K. Ohlendieck, Proteomic analysis of the sarcolemma-enriched fraction from dystrophic mdx-4cv skeletal muscle, *J. Proteomics*, 2019, **191**, 212–227.

47 P. Dowling, M. Zweyer, M. Raucamp, M. Henry, P. Meleady, D. Swandulla and K. Ohlendieck, Proteomic and cell biological profiling of the renal phenotype of the mdx-4cv mouse model of Duchenne muscular dystrophy, *Eur. J. Cell Biol.*, 2020, **99**, 151059.

48 S. Murphy, P. Dowling, M. Zweyer, D. Swandulla and K. Ohlendieck, Proteomic profiling of giant skeletal muscle protein, *Expert Rev. Proteomics*, 2019, **16**, 241–256.

49 S. Murphy, P. Dowling, M. Zweyer, M. Henry, P. Meleady, R. R. Mundegar, D. Swandulla and K. Ohlendieck, Proteomic profiling of mdx-4cv serum reveals highly elevated levels of the inflammation-induced plasma marker haptoglobin in muscular dystrophy, *Int. J. Mol. Med.*, 2017, **39**, 1357–1370.

50 S. Carberry, H. Brinkmeier, Y. Zhang, C. K. Winkler and K. Ohlendieck, Comparative proteomic profiling of soleus, extensor digitorum longus, flexor digitorum brevis and interosseus muscles from the mdx mouse model of Duchenne muscular dystrophy, *Int. J. Mol. Med.*, 2013, **32**, 544–556.

51 S. Rayavarapu, W. Coley, E. Cakir, V. Jahnke, S. Takeda, Y. Aoki, H. Grodish-Dressman, J. K. Jaiswal, E. P. Hoffman, K. J. Brown, Y. Hathout and K. Nagaraju, Identification of disease specific pathways using in vivo SILAC proteomics in dystrophin deficient mdx mouse, *Mol. Cell. Proteomics*, 2013, **12**, 1061–1073.

52 A. Holland, P. Dowling, P. Meleady, M. Henry, M. Zweyer, R. R. Mundegar, D. Swandulla and K. Ohlendieck, Label-free mass spectrometric analysis of the mdx-4cv diaphragm identifies the matricellular protein periostin as a potential factor involved in dystrophinopathy-related fibrosis, *Proteomic*, 2015, **15**, 2318–2331.

53 S. Murphy, M. Zweyer, M. Raucamp, M. Henry, P. Meleady, D. Swandulla and K. Ohlendieck, Proteomic profiling of the mouse diaphragm and refined mass spectrometric analysis of the dystrophic phenotype, *J. Muscle Res. Cell Motil.*, 2019, **40**, 9–28.

54 Y. Hathout, R. L. Marathi, S. Rayavarapu, A. Zhang, K. J. Brown, H. Seol, H. Gordish-Dressman, S. Cirak, L. Bello, K. Nagaraju, T. Partridge, E. P. Hoffman, S. Takeda, J. K. Mah, E. Henricson and C. McDonald, Discovery of serum protein biomarkers in the mdx mouse model and cross-species comparison to Duchenne muscular dystrophy patients, *Hum. Mol. Genet.*, 2014, **23**, 6458–6469.

55 S. Guiraud, B. Edwards, S. E. Squire, A. Babbs, N. Shah, A. Berg, H. Chen and K. E. Davies, Identification of serum protein biomarkers for utrophin based DMD therapy, *Sci. Rep.*, 2017, **7**, 43697.

56 A. Holland, P. Dowling, M. Zweyer, D. Swandulla, M. Henry, M. Clynes and K. Ohlendieck, Proteomic profiling of

cardiomyopathic tissue from the aged mdx model of Duchenne muscular dystrophy reveals a drastic decrease in laminin, nidogen and annexin, *Proteomics*, 2013, **13**, 2312–2323.

57 S. Murphy, H. Brinkmeier, M. Krautwald, M. Henry, P. Meleady and K. Ohlendieck, Proteomic profiling of the dystrophin complex and membrane fraction from dystrophic mdx muscle reveals decreases in the cytolinker desmoglein and increases in the extracellular matrix stabilizers biglycan and fibronectin, *J. Muscle Res. Cell Motil.*, 2017, **38**, 251–268.

58 F. Cynthia Martin, M. Hiller, P. Spitali, S. Oonk, H. Dalebout, M. Palmblad, A. Chaouch, M. Guglieri, V. Straub, H. Lochmüller, E. H. Niks, J. J. Verschuuren, A. Aartsma-Rus, A. M. Deelder, Y. E. van der Burgt and P. A. 't Hoen, Fibronectin is a serum biomarker for Duchenne muscular dystrophy, *Proteomics Clin Appl*, 2014, **8**, 269–728.

59 L. O. Chavez, M. Leon, S. Einav and J. Varon, Beyond muscle destruction: a systematic review of rhabdomyolysis for clinical practice, *Crit. Care*, 2016, **20**, 135.

60 K. Rodríguez-Capote, C. M. Balion, S. A. Hill, R. Cleve and L. Yang, A. El Sharif, Utility of urine myoglobin for the prediction of acute renal failure in patients with suspected rhabdomyolysis: a systematic review, *Clin. Chem.*, 2009, **55**, 2190–2197.

61 D. R. Scoles and S. M. Pulst, Antisense therapies for movement disorders, *Mov. Disord*, 2019, **34**, 1112–1119.

62 C. S. Young, A. D. Pyle and M. J. Spencer, CRISPR for Neuromuscular Disorders: Gene Editing and Beyond, *Physiology*, 2019, **34**, 341–353.

63 C. Sun, C. Serra, G. Lee and K. R. Wagner, Stem cell-based therapies for Duchenne muscular dystrophy, *Exp. Neurol.*, 2020, **323**, 113086.

64 M. A. Waldrop and K. M. Flanigan, Update in Duchenne and Becker muscular dystrophy, *Curr. Opin. Neurol.*, 2019, **32**, 722–727.

65 M. Thangarajh, A. Zhang, K. Gill, H. W. Ressom, Z. Li, R. S. Varghese, E. P. Hoffman, K. Nagaraju, Y. Hathout and S. M. Boca, Discovery of potential urine-accessible metabolite biomarkers associated with muscle disease and corticosteroid response in the mdx mouse model for Duchenne, *PLoS One*, 2019, **14**, e0219507.

66 S. Murphy, M. Zweyer, R. R. Mundegar, D. Swandulla and K. Ohlendieck, Proteomic identification of elevated saliva kallikrein levels in the mdx-4cv mouse model of Duchenne muscular dystrophy, *Biochem. Biophys. Rep.*, 2018, **18**, 100541.

67 B. S. Antharavally, K. A. Mallia, P. Rangaraj, P. Haney and P. A. Bell, Quantitation of proteins using a dye-metal-based colorimetric protein assay, *Anal. Biochem.*, 2009, **385**, 342–345.

68 V. Urquidi, M. Chang, Y. Dai, J. Kim, E. D. Wolfson, S. Goodison and C. J. Rosser, IL-8 as a urinary biomarker for the detection of bladder cancer, *BMC Urol.*, 2012, **12**, 12.

69 J. R. Wiśniewski, Filter-Aided Sample Preparation: The Versatile and Efficient Method for Proteomic Analysis, *Methods Enzymol.*, 2017, **585**, 15–27.

70 R. Aebersold and M. Mann, Mass-spectrometric exploration of proteome structure and function, *Nature*, 2016, **537**, 347–355.

71 S. Anand, M. Samuel, C. S. Ang, S. Keerthikumar and S. Mathivanan, Label-Based and Label-Free Strategies for Protein Quantitation, *Methods Mol. Biol.*, 2017, **1549**, 31–43.

72 J. A. Ankney, A. Muneer and X. Chen, Relative and Absolute Quantitation in Mass Spectrometry-Based Proteomics, *Annu. Rev. Anal. Chem.*, 2018, **11**, 49–77.

73 D. A. Megger, L. L. Pott, M. Ahrens, J. Padden, T. Bracht, K. Kuhlmann, M. Eisenacher, H. E. Meyer and B. Sitek, Comparison of label-free and label-based strategies for proteome analysis of hepatoma cell lines, *Biochim. Biophys. Acta*, 2014, **1844**, 967–976.

74 A. Latosinska, K. Vougas, M. Makridakis, J. Klein, W. Mullen, M. Abbas, K. Stravodimos, I. Katafigiotis, A. S. Merseburger, J. Zoidakis, H. Mischak, A. Vlahou and V. Jankowski, Comparative Analysis of Label-Free and 8-Plex iTRAQ Approach for Quantitative Tissue Proteomic Analysis, *PLoS One*, 2015, **10**, e0137048.

75 H. Mi, A. Muruganujan, D. Ebert, X. Huang and P. D. Thomas, PANTHER version 14: more genomes, a new PANTHER GO-slim and improvements in enrichment analysis tools, *Nucleic Acids Res.*, 2019, **47**(D1), D419–D426, DOI: 10.1093/nar/gky1038, 30407594.

76 D. Szklarczyk, A. L. Gable, D. Lyon, A. Junge, S. Wyder, J. Huerta-Cepas, M. Simonovic, N. T. Doncheva, J. H. Morris, P. Bork, L. J. Jensen and C. von Mering, STRING v11: protein-protein association networks with increased coverage, supporting functional discovery in genome-wide experimental datasets, *Nucleic Acids Res.*, 2019, **47**(D1), D607–D613, DOI: 10.1093/nar/gky1131, 30476243.

